

A study of quantum decoherence in a system with Kolmogorov-Arnol'd-Moser tori

G. H. Ball, K. M. D. Vant, H. Ammann and N. L. Christensen
Department of Physics, University of Auckland, Auckland, New Zealand

June 19, 2021

Abstract

We present an experimental and numerical study of the effects of decoherence on a quantum system whose classical analogue has Kolmogorov-Arnol'd-Moser (KAM) tori in its phase space. Atoms are prepared in a caesium magneto-optical trap at temperatures and densities which necessitate a quantum description. This real quantum system is coupled to the environment via spontaneous emission. The degree of coupling is varied and the effects of this coupling on the quantum coherence of the system are studied. When the classical diffusion through a partially broken torus is $\lesssim \hbar$, diffusion of quantum particles is inhibited. We find that increasing decoherence via spontaneous emission increases the transport of quantum particles through the boundary.

1 Introduction

The study of decoherence in a quantum system has been a subject of much interest in recent years. Since the emergence of quantum mechanics some seventy years ago, a central problem in its interpretation has been the fact that the linearity of the Schrödinger equation allows macroscopic physical states to be derived from arbitrary superpositions of other states, a situation which is quite clearly in contradiction to our experience. This was originally illustrated in the familiar paradox of Schrödinger's cat. One simple explanation is to suppose that an initially classical state for a macroscopic system will always evolve into another classical state so that for a universe with a suitable initial condition, non-classical states occur only when carefully prepared by some experimentalist. In this interpretation Schrödinger's cat

presents no paradox, but merely lies outside our normal realm of experience. This hypothesis can be rejected in the light of quantum analysis of real macroscopic, classically chaotic systems. Calculations (see for example Zurek's discussion in terms of celestial objects [1]) indicate that in these systems, quantum dynamics differ from classical after relatively short times, and lead to flagrantly non-classical states. Any successful theory must explain why these states are not found in practice.

There have been several more sophisticated explanations as to why quantum states are not evident in our everyday world. The first was Neils Bohr's Copenhagen Interpretation (CI) [2]. Bohr theorized that quantum theory was not universal — a classical apparatus was necessary to carry out the measurements. He also required that the boundary between quantum and classical domains was mobile and could be pushed back by appropriate apparatus. Another significant school of thought was Hugh Everett's Many World's Interpretation (MWI) [3, 4]. He proposed that each time an interaction which would produce a superposition takes place, the wave-function of the universe bifurcates to give an ever increasing number of 'branches'. In 1952, David Bohm [5] detailed an interpretation based on 'hidden' variables which had previously been investigated to some extent by de Broglie [6]. Bohm theorized that these hidden variables would allow "a detailed causal and continuous description of all processes, and not require us to forego the possibility of conceiving the quantum level in precise terms." Many other approaches to the problem have been taken, examples of which can be found in [7-9].

A more recent and arguably more satisfactory solution to the problem of quantum-classical correspondence has been championed by Wojciech Zurek and co-workers [10, 11]. They suggest that any real, open quantum system leaks coherence to its surroundings via extraneous degrees of freedom which are coupled to the environment. A suitable environment might be provided by air molecules, cosmic background microwave photons, or the vacuum point fluctuations of the electromagnetic field. The rate at which this decoupling proceeds depends on the particular state of the system, the dynamics of the system and the form of the interaction with the environment. The states most resistant to decoherence form a (not necessarily orthogonal) basis of 'pointer' states which are 'selected'; the density matrix rapidly becomes diagonal in this basis [12]. Any particular realization of the system quickly evolves into one of these basis states, and only measurements in this basis can be thought of as revealing the true state of the system. It appears to be a general result that the "pointer" states are the "most classical" states of the system. In most cases for macroscopic systems

the pointer states are expected to be those which are localized to a high degree. This arises from the fact that in most cases the system's interactions with the environment are chiefly position dependent. Superpositions of the pointer states of a system will collapse on a time scale determined by the coupling. In a measurement of a microscopic system by a macroscopic observer, the wave-function collapse of traditional measurement theory is caused by decoherence of the meter entangled with the system. Bizarre macroscopic quantum states might in theory be prepared, but will survive only for a vanishingly short time, and the classical description of the world as we observe it will be regained. Quantum mechanics without fundamental modification retains its position as the true description of the universe, and the limited set of states which we observe around us is accounted for.

In this paper, we study experimentally the effects of increasing the coupling of a quantum system to its environment. Our experimental system is a low density cloud of super cool ($\sim 15\mu K$) caesium atoms prepared in the ultra high vacuum glass cell of a magneto-optical trap (MOT). Because of the low densities achieved in a MOT, the interactions of the atoms are negligible and each atom can be modeled as a quantum particle in a periodic potential (see Section 3). With 10^5 atoms trapped per experimental run, we deal with statistically significant numbers of particles so the experimental distributions will closely approximate quantum probability distributions. We temporally modulate a standing wave optical potential which then creates Kolmogorov-Arnol'd-Moser (KAM) tori (impenetrable momentum barriers) in the classical phase space of the system. For an increased Rabi frequency (i.e. increased perturbation), holes appear in the barriers, now called cantori, through which the atoms can diffuse. The diffusion rates of classical and quantum particles are distinctly different, with quantum diffusion being largely suppressed by the cantori. The decohering effects of coupling to the environment bring the behaviour of the quantum ensemble towards the classical limit.

2 The Kolmogorov-Arnol'd-Moser Theorem

For a closed system with an integrable Hamiltonian, all solutions lie on two dimensional tori embedded in $2N - 1$ dimensional phase space, where N is the number of degrees of freedom of the system. Each solution or trajectory is indefinitely confined to its own torus. The motion of a trajectory on a torus can be described by two coordinates, θ_1 and θ_2 on $[0, 2\pi)$. The winding

number w of the torus is defined as

$$w = \frac{\omega_1}{\omega_2}, \text{ where } \omega_j = \dot{\theta}_j, \text{ for } j = 1, 2. \quad (1)$$

If the two frequencies ω_j are commensurate then the winding number of the torus is rational, and trajectories on the torus are periodic. If the frequencies are incommensurate the winding number is irrational, and the motion in phase space is quasi-periodic.

When the system Hamiltonian is perturbed such that it becomes non-integrable, non-linear resonances appear in the phase space at the location of tori with rational winding numbers, altering the topology and destroying these tori (see Section 3). Trajectories which were confined on the vanished tori, now traverse the same general region of phase space. However the KAM theorem states that tori with irrational winding numbers (KAM tori) are not immediately destroyed by small amounts of non-integrability and continue to act as tori in the new phase space. For increasing perturbation, the non-linear resonances grow and the KAM tori are eventually destroyed by nearby resonances. Within a given region of phase space, those with the most irrational winding numbers are the last to break up. Irrationality is measured by the rate of convergence of the continued fraction representation,

$$w \equiv [a_0, a_1, a_2, \dots] = a_0 + \frac{1}{a_1 + \frac{1}{a_2 + \frac{1}{a_3 + \dots}}} \quad (2)$$

When a KAM torus is destroyed, a *cantorus* is left in its place. The properties of a broken torus or cantorus in a quantum system have been the subject of considerable interest and several numerical studies [13–17].

3 Our analytical system

The atom interacts with a standing wave of near-resonant light (frequency ω_L) which is temporally modulated with period T . When the detuning $\delta_L = \omega_0 - \omega_L$ (where ω_0 is the resonant frequency of the transition) is sufficiently large compared to the resonant Rabi frequency $\Omega/2$ (proportional to the square root of the standing wave intensity), the amplitudes of the excited states can be adiabatically eliminated. The dynamics are governed by stimulated two-photon scattering between ground states, with momentum changes in units of $2\hbar k_L$. Classically the atom behaves as a dipole in

a conservative one dimensional potential. The Hamiltonian in this limit is given by

$$\mathcal{H} = \frac{p_x^2}{2M} - \frac{\hbar\Omega_{\text{eff}}}{8} \cos 2k_L x \sum_{n=-\infty}^{\infty} f\left(\frac{t}{T} - n\right) \quad (3)$$

where $f(t/T)$ specifies the temporal shape of the “kicks,” (with $0 \leq f(t/T) \leq 1$), k_L is the laser wave number, and Ω_{eff} is the effective Rabi frequency. For a two-level atom $\Omega_{\text{eff}} = \Omega^2/\delta_L$ but for our system we instead have $\Omega_{\text{eff}} = \Omega^2(s_{45}/\delta_{45} + s_{44}/\delta_{44} + s_{43}/\delta_{43})$, where the terms in brackets take into account the different dipole transitions between the relevant hyperfine levels in caesium ($F = 4 \rightarrow F' = 5, 4, 3$). In our simulations we assumed equal populations of the Zeeman sub-levels, yielding numerical values for the s_{4j} of $s_{45} = 11/27$, $s_{44} = 7/36$, and $s_{43} = 7/108$; δ_{4j} are the corresponding detunings. Note that the different magnetic sub-levels will experience different AC Stark shifts. For the smallest detuning used in this work this results in a 5% spread in the coupling strength.

We can write the Hamiltonian in dimensionless form as

$$H = \frac{\rho^2}{2} - k \cos \phi \sum_{n=-\infty}^{\infty} f(\tau - n) \quad (4)$$

where $k = \hbar\Omega_{\text{eff}}k_L^2T^2/2M$ is a measure of the perturbation of the system called the kick strength, $\tau = t/T$, $\phi = 2k_Lx$, $\rho = (2k_LT/M)p_x$, and $H = (4k_L^2T^2/M)\mathcal{H}$. If we consider the dynamics on a single half wavelength of the laser beam, the Hamiltonian is that of a driven rotor, with dimensionless parameters $I = 1$ and $\omega_0^2 = k$, where ω_0 is the small amplitude oscillation frequency of the rotor. In the quantized model, ϕ and ρ are conjugate variables with a commutation relation $[\rho, \phi] = -i\hbar$, where $\hbar = 4\hbar k_L^2T^2/M$ is our scaled Planck constant.

Experimentally, we use a double pulse kick (see Figure 1 and Section 4). For this $f(\tau)$ the Hamiltonian can alternatively be written as

$$H = \frac{\rho^2}{2} - k \sum_{m=-\infty}^{\infty} a_m \cos(\phi - 2\pi m\tau) \quad (5)$$

where $a_m = \frac{1}{10} \text{sinc} \frac{m\pi}{20} \cos \frac{m\pi}{10}$. (With the sinc function defined as $\text{sinc}(x) = \sin(x)/x$). The rotor is driven by traveling cosine waves, the speed of the m^{th} cosine wave corresponding to a dimensionless momentum of $\rho = 2\pi m$. There will be a primary resonance in the phase space wherever the speed of

rotation of the rotor matches the speed of a cosine wave [18]. In the reference frame in which the cosine wave is at rest, the rotor will be trapped in a pendulum potential. This causes a change in the topology of the classical phase space at $\rho = \rho_m$, for $a_m \neq 0$. For m such that $a_m = 0$ there is a missing primary resonance. The widths of the primary resonance zones are given by $\delta\rho_m = 4\sqrt{a_mk}$. The Chirikov condition for overlap is that the spacing between the resonances be equal to the sum of the half-widths or $|\rho_m - \rho_n| = 2\sqrt{a_mk} + 2\sqrt{a_nk}$. Overlap of adjacent resonances is the mechanism for the destruction of KAM tori. We expect tori in the vicinity of missing resonances to survive higher kick strengths than all others. A more sophisticated analysis must take into account the appearance of secondary resonances arising from interactions between the primary resonances.

4 Experimental Set-up

Our experimental setup is very similar to that used in the experiments of Ammann *et al* [19, 20] and Moore *et al* [21]. Approximately 10^5 caesium atoms are trapped and laser cooled in a standard MOT powered by two diode lasers operating in the infra-red (852nm). The initial trapped cloud has a FWHM of $\sim 200\mu m$ and a temperature of $10-15\mu K$. The periodically modulated potential (described in Section 3) is provided by a third diode laser. The beam from this laser passes through an 80MHz acousto-optic modulator (AOM) and a single mode optical fibre which spatially filters the light and delivers it to the trap. The beam is then collimated and retro-reflected from a mirror on the opposite side of the trap to form a standing wave potential across the atomic cloud. The calculated beam waist at the cloud is $795\mu m$. This potential is temporally modulated via the rf supply to the AOM. Our calculated Rabi frequency at the centre of the trap, for maximum optical power is $\Omega/2\pi = 310 MHz$. A reasonably narrow distribution in the kicking strength k is produced by the finite widths of the cloud and the beam waist of the kicking potential (RMS spread of 6% and $k_{mean} \approx 0.94k_{max}$). In the remainder of this paper, k always refers to k_{mean} .

In the system Hamiltonian, the pulse train is described by $f(\tau)$. Any pulse of finite length will create KAM tori in the phase space of the system. These impenetrable barriers to diffusion were observed in recent quasi δ -kicked rotor experiments [19, 20, 22] and were discussed in a recent paper by Klappauf *et al* [23]. In these studies the effects of the boundaries were avoided by tailoring the pulse length to push them into regions of phase space beyond the localization length of dynamical localization. However,

they present a very interesting area of study in themselves and have been investigated both numerically and experimentally [13–17, 24, 25]. A pulse train consisting of single pulses is not the best system for studying KAM tori because the only energetic chaotic sea lies within the tori of lowest momentum. Energetic chaotic seas aid the diffusion of particles away from the partially permeable barrier and are important experimentally in isolating the effect of the boundary in phase space. We use a double pulse per kicking cycle where the pulse period is $T = 25\mu s$ with pulse width $\alpha = 1/20$ and pulse spacing $\Delta = 1/10$ (see Figure 1). This pulse shape gives energetic chaotic seas on both sides of the long-lived KAM tori with the smallest absolute momentum (see Figure 2). To achieve varying levels of spontaneous emission, we varied $\delta_L = \omega_0 - \omega_L$, the detuning of the kicking potential from resonance, while simultaneously altering the beam intensity to maintain a constant kicking strength.

5 Transport through cantori

Classical particles which are no longer confined to their own tori can diffuse rapidly even through a recently broken cantorus. The cantorus no longer forms an impenetrable barrier in the classical phase space and trajectories from both sides of the original boundary can eventually fill the entire region between two adjacent, unbroken tori. For quantum particles however, a very different behaviour had been predicted. Various numerical studies of particle transport through cantori [13–17] suggested that until the phase space area escaping through the cantori per kick cycle was $\sim \hbar$, the diffusion of quantum particles would be restricted to a quantum tunnelling like behaviour. Hence the prediction was for a distinct difference between the diffusion rates of classical and quantum particles. Figure 2a shows a Poincare section of our system for a very low kicking strength. The KAM tori at $\rho = \pm 10\pi$ and $\pm 30\pi$ are clearly visible as regions of stability between large chaotic seas. Figure 2b shows the Poincare section for $k \sim 300$, which is comparable to the kicking strengths used in our experimental work. The tori at $\rho = \pm 10\pi$ are no longer visible in the phase space at this resolution; however they have been shown to still have a significant effect on the dynamics of both the quantum [24, 25] and classical systems.

We prepare our atoms so that they initially lie within the $\rho = \pm 10\pi$ cantori and monitor their subsequent evolution through the boundary. The final momentum distributions of the atomic cloud display distinctive ‘shoulders’ at $\rho = \pm 10\pi$ (as shown in Figure 3) due to the inhibition of diffusion

introduced by the cantori. This KAM localization is distinct from the more widely studied ‘dynamical localization’. The signature of dynamical localization is an exponential lineshape in momentum space which is markedly different from the box-like distributions and characteristic shoulders observed with KAM boundaries. Also, for this experiment, the localization length of the system, $l_\rho \sim 170$ is considerably longer than the momentum width of the 1st and 2nd KAM boundaries at $\rho = \pm 10\pi$ and $\pm 30\pi$ and hence KAM localization occurs before dynamical localization can have an effect.

6 Decoherence

The theory of decoherence provides the most recent and so far perhaps the most satisfying of a series of attempts to explain the disparities between the predictions of quantum mechanics and the everyday experiences of the world we inhabit (see Section 1). The field of quantum chaos provides an ideal backdrop for a study of the predicted effects of decoherence. It is now widely accepted that sensitive dependence on initial conditions - the hallmark of classical chaos - does not occur in closed quantum systems. This raises problems for the quantum-classical correspondence (QCC) principle. Quantum mechanics must be able to describe the classical limit of chaotic behaviour. In this case, employing the limit as $\hbar \rightarrow 0$ is not entirely satisfactory. Chaotic systems can develop highly complex phase space structures in logarithmically short times and hence the small but non-zero value of \hbar is an important factor.

According to the work of Zurek *et al* [10, 11], these difficulties in restoring the classical behaviour can be eliminated by realizing that it is not possible to isolate macroscopic quantum systems from their environment. The coupling of the extraneous degrees of freedom of a system to the environment destroys the quantum coherences on a time scale inversely proportional to the degree of coupling. In our experiments and simulations, we introduce coupling via spontaneous emission induced by the kicking potential. As the level of spontaneous emission increases so does the coupling of the system to the vacuum fluctuations which constitute the environment. The predicted effect of this increasing coupling is an increase in the transport of quantum particles across the cantori as the quantum diffusion rate tends to its classical limit.

For the purposes of simulation we note that $H = \rho^2/2 - k \cos \phi = H_{\text{light}}$ while the driving potential is ‘switched on’, and $H = \rho^2/2 = H_{\text{dark}}$ otherwise. Classical trajectories involve periods of pendulum motion described by Jacobi elliptic functions, alternating with periods of free evolution. Usually

10^4 trajectories are followed during each run. For each pulse, the amplitude and phase of the elliptic function is matched to the position and motion of each trajectory by inverting the elliptic function numerically. To simulate our experiments, we choose a thermal random distribution of initial conditions. To produce Poincare sections, more uniform conditions are chosen, and optimized to reveal the phase space structure.

The quantum system is represented by a basis of $N = 128$ momentum eigenstates $|n\rangle$, where $\rho|n\rangle = n\hbar|n\rangle$ and $n = -64, \dots, 63$. The evolution operator for a single kick is

$$U = \exp(-i\frac{17H_{\text{dark}}}{40\hbar}) \exp(-i\frac{H_{\text{light}}}{20\hbar}) \exp(-i\frac{H_{\text{dark}}}{20\hbar}) \dots \\ \times \exp(-i\frac{H_{\text{light}}}{20\hbar}) \exp(-i\frac{17H_{\text{dark}}}{40\hbar}) \quad (6)$$

where $\langle m|H_{\text{dark}}|n\rangle = \frac{1}{2}n^2\hbar^2\delta_{m,n}$, $\langle m|H_{\text{light}}|n\rangle = \frac{1}{2}n^2\hbar^2\delta_{m,n} - \frac{1}{2}\hbar k(\delta_{m,n+1} + \delta_{m,n-1})$ and we treat n as periodic. The $N \times N$ matrices are exponentiated numerically. In the case of evolution without spontaneous emission, the evolution is entirely coherent, and is solved by finding the eigenvectors of the evolution operator (Floquet method). For incoherent evolution, the effects of spontaneous emission are simulated by adding the density matrix to two shifted versions of itself, once per kick:

$$\langle m|\hat{\mathcal{P}}|n\rangle = \frac{1}{2}\eta \left(\langle m+1|\hat{\mathcal{P}}|n+1\rangle + \langle m-1|\hat{\mathcal{P}}|n-1\rangle \right) + (1-\eta) \langle m|\hat{\mathcal{P}}|n\rangle \quad (7)$$

where $\hat{\mathcal{P}}$ is the density operator and η is the probability for a particular atom to spontaneously emit during one kick cycle.

A convenient way to visualize the information represented by the density matrix is in the form of a Wigner function. For a discrete, truncated basis we use the toroidal Wigner function as defined in [26].

$$w(X_k, P_l, t) = \sum_{j=0}^{2N-1} \exp\left(i\frac{\pi jk}{N}\right) \frac{1 + (-1)^{l+j}}{2} \left\langle \frac{l+j}{2} \left| \hat{\mathcal{P}} \right| \frac{l-j}{2} \right\rangle \quad (8)$$

Where $P_l = (\hbar/2)l$ and $X_k = \pi k/N$. This gives a Wigner function defined on a $2N \times 2N$ grid. Averaging over cells of four adjacent points we reduce the grid to $N \times N$. Examples of results obtained are shown in Figure 4. We see that decoherence smooths the Wigner function, removing the rapid oscillations and negative regions which are characteristic of quantum interference phenomena.

7 Experimental results

In the absence of decoherence the caesium atoms behave as quantum particles. Thus even for cantori where significant diffusion of classical particles can occur, our quantum particles should still be strongly contained as can be seen from our classical and quantum simulations in Figure 5 where we calculate the percentage of atoms that cross the $\rho = \pm 10\pi$ cantori as a function of the number of kick cycles. Not until the phase space escaping through the cantorus per cycle is $\sim \hbar$, or in our scaled units $\sim \tilde{\hbar}$, do the quantum particles move to any great extent across the boundary. For our experimental parameters, the phase space flux through the $\rho = \pm 10\pi$ cantori per kicking cycle is $\sim 4.6\tilde{\hbar}$ so the quantum diffusion will be strongly inhibited. The predicted effect of increasing the coupling to the environment then is to increase the transfer of atoms across the cantorus. As the quantum system becomes more and more strongly coupled to its environment, the behaviour of the atoms is expected to approach the classical limit of rapid diffusion.

Our experimental results support this prediction (see Figure 6). For a given kick strength, we tuned closer to resonance in steps from $\delta = 2.8GHz$. A lower limit on the detuning is imposed by the approximation made in our numerical calculations that the excited state of the atoms can be adiabatically eliminated (see Section 3). The upper limit ($2.8GHz$) is mainly due to optical power restrictions from our diode laser - as the detuning increases, the intensity must also increase to maintain a constant kicking strength. As the detuning decreased, the percentage of particles outside the 1st KAM boundary increased and the experimental curve rose towards the classical prediction. Our results also show reasonable agreement with our quantum mechanical simulations which included the effects of spontaneous emission. The main sources of error are the measurement of optical beam power and the finite resolution of the CCD camera.

8 Conclusion

Using laser-cooled caesium atoms, we have observed the controlled decoherence of a real quantum system via coupling to the environment. This adds to the previous work on decoherence through the atom optics realization of the δ -kicked rotor and also the experiments of Haroche *et al* [27] and Wineland *et al* [28]. We have demonstrated that the quantum diffusion rate tends towards the classical rate with an increasing degree of decoherence. The introduction of decoherence via spontaneous emission increases the rate

of transport of atoms across the cantori and alters the characteristic shape of the KAM localized distribution such that it tends towards the classical (uniform) distribution.

The link between the quantum domain and the familiar classical world remains a hotly debated topic. The quantum classical correspondence principle requires that quantum mechanics contains the classical macroscopic limit. Taking $\hbar \rightarrow 0$ is not a realistic strategy in the laboratory. The physical effects of a very small, but definitely non-zero, \hbar manifest themselves in chaotic systems through highly complex phase space structures of order $\sim \hbar$ that develop in logarithmically short times $\sim \ln(1/\hbar)$. It appears that only through environment induced decoherence can the quantum — classical correspondence principle be justified. This interpretation is authenticated via the results presented in this present paper, as well as our group’s previous study of decoherence in the atomic optics manifestation of the delta kicked rotor [19, 20]. While we can make our ensemble of Cs atoms behave like an ensemble of classical particles, we do not infer that there is any degree of chaos in the presented quantum system. Everything happening to our atoms is intrinsically quantum mechanical, but through the slight phase shift that an atom’s wavefunction acquires when it recoils from the spontaneous emission absorption — emission cycle the momentum localization is destroyed. This process can be observed and understood in the laboratory, or through Monte Carlo wavefunction [19] or density of state calculations. We can track our theoretical atom’s momentum wavefunction as it absorbs and re-emits environmental photons, and through this process localization is eliminated and diffusion similar to that predicted classically is observed. It is still all quantum mechanics; the physical coupling to the environment produced behaviour that only “appears” classical.

Acknowledgements

This work was supported by the Royal Society of New Zealand Marsden Fund and the University of Auckland Research Committee. The authors would like to thank Dan Walls and other members of the University of Auckland Quantum Optics group for useful discussions, guidance and encouragement throughout the course of this research.

References

- [1] W. H. Zurek, Preprint quant-ph/9802054 (1998).
- [2] N. Bohr, Nature **121**, 580 (1928).
- [3] H. Everett III, Review of Modern Physics **29**, 454 (1957).
- [4] J. A. Wheeler, Review of Modern Physics **29**, 463 (1957).
- [5] D. Bohm, Physical Review **85**, 166 (1952).
- [6] L. de Broglie, *An Introduction to the Study of Wave Mechanics* (E P Dutton and Company, Inc., New York, 1930).
- [7] *Quantum Theory and Measurement* edited by J.A. Wheeler and W.H. Zurek, Princeton Series in Physics, Princeton University Press, 1983.
- [8] W. L. Power and I. C. Percival, Preprint quant-ph/9811059 (1998).
- [9] R. Penrose, General Relativity and Gravitation **28**, 581 (1994).
- [10] W. H. Zurek and J. P. Paz, Physical Review Letters **72**, 2508 (1994).
- [11] W. H. Zurek, Physics Today **44**, 36 (1991).
- [12] J. P. Paz and W. H. Zurek, Preprint quant-ph/9811026 (1998).
- [13] T. Geisel, G. Radons, and J. Rubner, Physical Review Letters **57**, 2883 (1986).
- [14] T. Geisel and G. Radons, Physica Scripta **40**, 340 (1989).
- [15] R. C. Brown and R. E. Wyatt, Physical Review Letters **57**, 1 (1986).
- [16] R. S. MacKay and J. D. Meiss, Physical Review A **37**, 4702 (1988).
- [17] R. S. MacKay, J. D. Meiss, and I. C. Percival, Physica D **13D**, 55 (1984).
- [18] L. E. Reichl, *The Transition to Chaos In Conservative Classical Systems: Quantum Manifestations*, Institute for Nonlinear Science (Springer-Verlag, New York, 1992).
- [19] H. Ammann, R. Gray, I. Shvarchuck, and N. Christensen, Physical Review Letters **80**, 4111 (1998).

- [20] H. Ammann, R. Gray, N. Christensen, and I. Shvarchuck, *Journal of Physics B: Atomic, Molecular and Optical Physics* **31**, 2449 (1998).
- [21] F. L. Moore *et al.*, *Physical Review Letters* **73**, 2974 (1994).
- [22] F. L. Moore *et al.*, *Physical Review Letters* **75**, 4598 (1995).
- [23] B. G. Klappauf, W. H. Oskay, D. A. Steck, and M. G. Raizen, *Physica D*, In press (1998).
- [24] N. Christensen, H. Ammann, G. Ball, and K. Vant, *Laser Physics*, In press (1998).
- [25] K. Vant, G. Ball, H. Ammann, and N. Christensen, *Physical Review E*, In press (1998).
- [26] A. R. Kolovsky, *Chaos* **6**, 534 (1996).
- [27] M. Brune *et al.*, *Physical Review Letters* **77**, 4887 (1996).
- [28] C. Monroe, D. M. Meekhof, B. E. King, and D. J. Wineland, *Science* **272**, 1131 (1996).

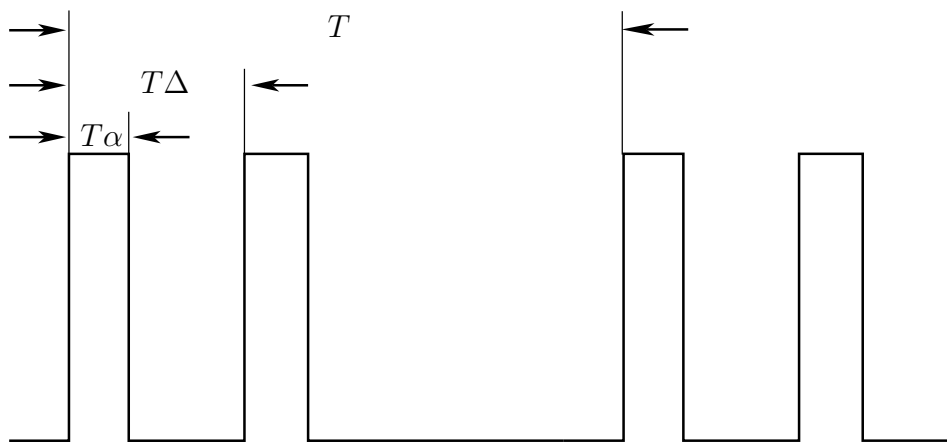


Figure 1: Double pulse showing definitions of α and Δ

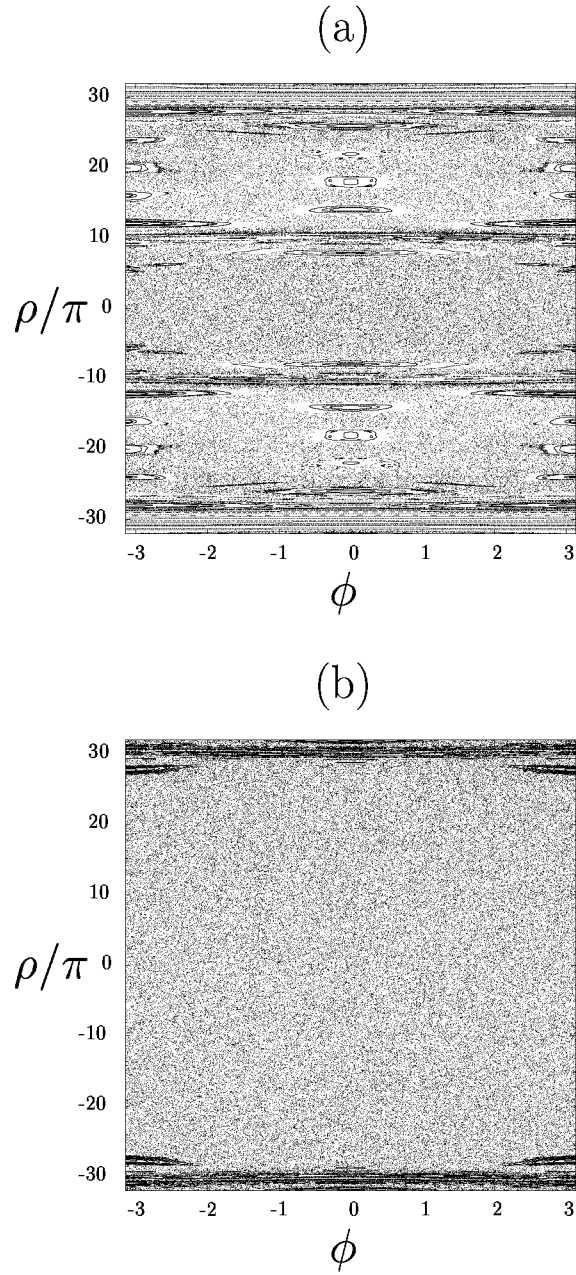


Figure 2: (a) is the Poincare section of the system for a very low kick strength. The unbroken KAM tori are clearly visible at $\rho = \pm 10\pi$ and $\pm 30\pi$, (b) shows the same Poincare section for $k \sim 300$ where the cantori at $\rho = \pm 10\pi$ have completely vanished from the phase space

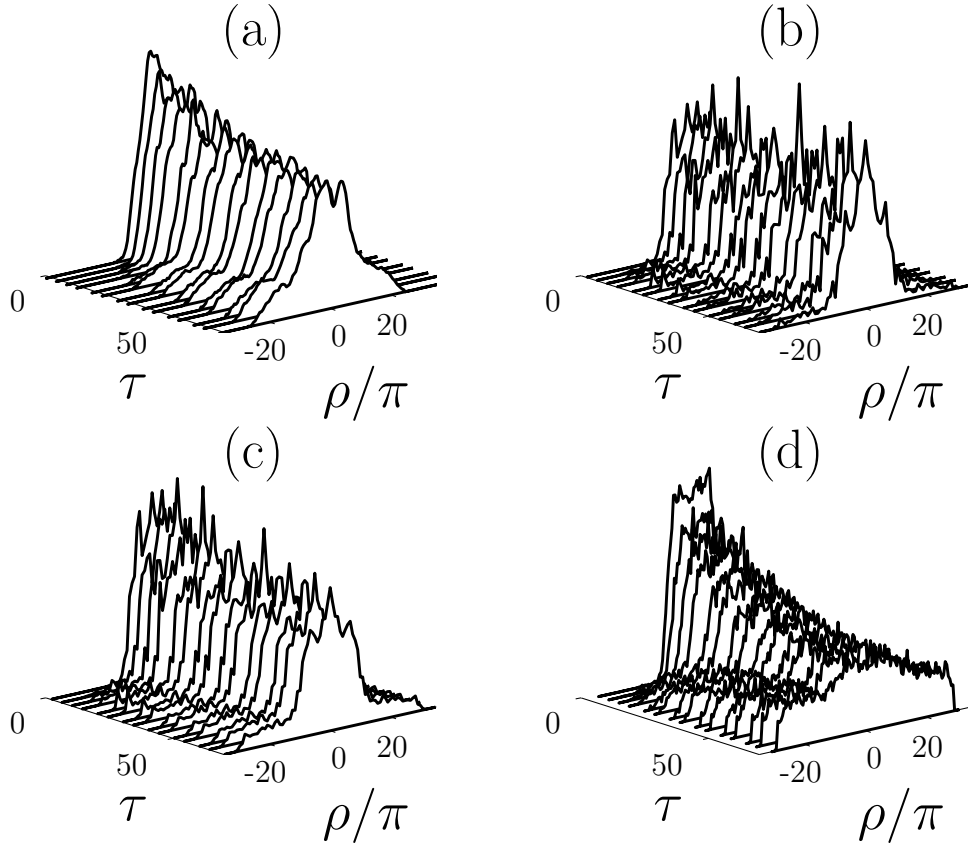


Figure 3: Momentum distributions for a kick strength $k = 280$ as a function of the number of kicking cycles τ . The experimental data (a) with its probability of spontaneous emission per cycle $\eta = 1.9\%$, shows its distinctive shoulders at $\rho = \pm 10\pi$. (b) is a quantum simulation for the experimental parameters with no spontaneous emission, (c) is a quantum simulation including spontaneous emission $\eta = 1.9\%$ and (d) shows the corresponding classical simulation.

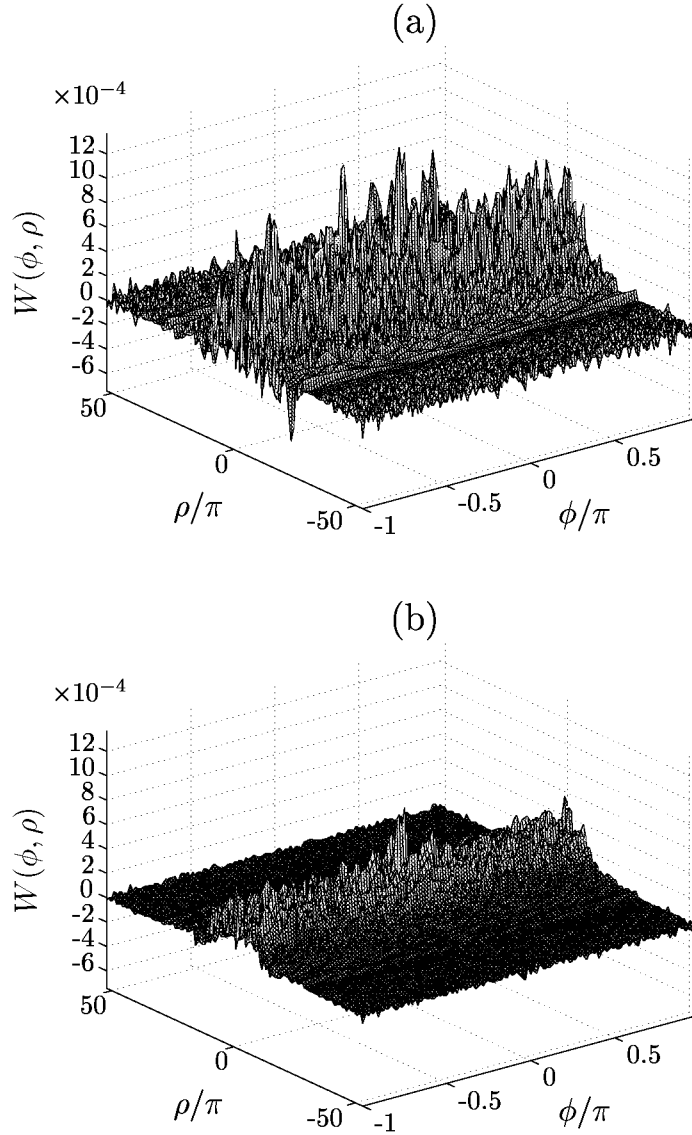


Figure 4: Wigner functions for the system after 70 kicks, with $k = 280$. (a) corresponds to a probability of spontaneous emission per kick cycle $\eta = 0\%$, giving pure quantum evolution. We see rapid fluctuations and negative regions, indicating quantum interference effects. (b) shows results for $\eta = 2\%$, comparable to experimental value. Quantum effects are reduced leading to a more classical distribution.

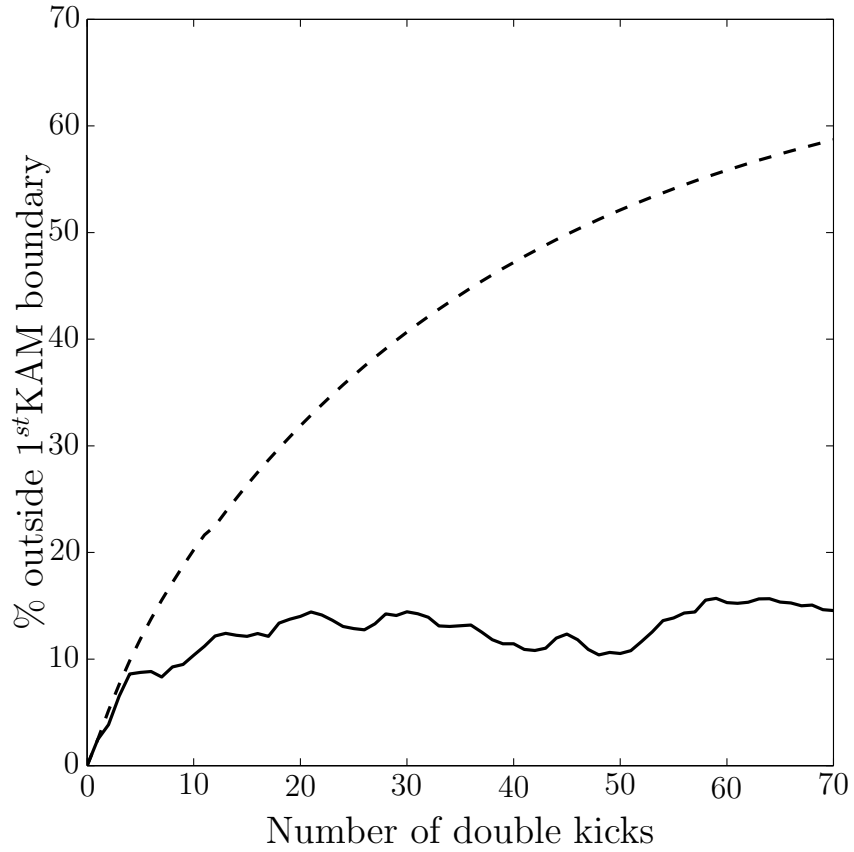


Figure 5: Quantum (solid) and Classical (dashed) simulations for a kicking strength of $k = 270$ showing the percentage of atoms to cross the $\rho = \pm 10\pi$ cantori. This graph clearly shows the inhibition to quantum diffusion presented by the cantorus.

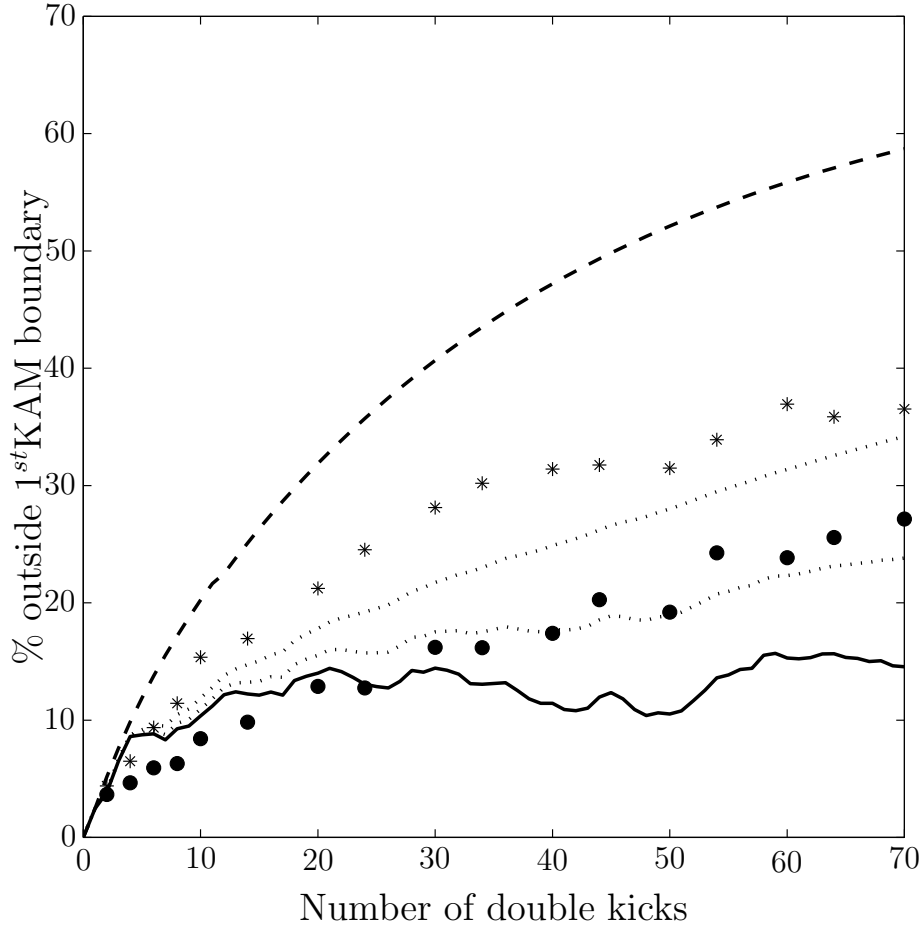


Figure 6: Percentage of particles to cross the $\rho = \pm 10\pi$ cantori. Experimental results for $\eta = 0.0187$ (\bullet) and $\eta = 0.0503$ (\circ) all at a kicking strength of $k = 270$. Quantum simulations for the experimental parameters are shown as dotted lines. The classical simulation (dashed) and quantum simulation with zero spontaneous emission (solid) are shown for comparison